

Moment domain representation of nonblind image deblurring

Ahmad Kumar,* Raveendran Paramesran, and Barmak Honarvar Shakibaei

Department of Electrical Engineering, University of Malaya, 50603 Kuala Lumpur, Malaysia

*Corresponding author: kumarahlad@gmail.com

Received 4 November 2013; revised 30 January 2014; accepted 30 January 2014;
posted 30 January 2014 (Doc. ID 200455); published 7 March 2014

In this paper, we propose the use of geometric moments to the field of nonblind image deblurring. Using the developed relationship of geometric moments for original and blurred images, a mathematical formulation based on the Euler–Lagrange identity and variational techniques is proposed. It uses an iterative procedure to deblur the image in moment domain. The theoretical framework is validated by a set of experiments. A comparative analysis of the results obtained using the spatial and moment domains are evaluated using a quality assessment method known as the Blind/Reference-less Image Spatial Quality Evaluator (BRISQUE). The results show that the proposed method yields a higher quality score when compared with the spatial domain method for the same number of iterations. © 2014 Optical Society of America

OCIS codes: (100.1830) Deconvolution; (100.2960) Image analysis; (100.2980) Image enhancement; (100.1455) Blind deconvolution.

<http://dx.doi.org/10.1364/AO.53.00B167>

1. Introduction

Deblurring is often termed as an inverse problem, in which the perceived blurred image, $g(x, y)$ is modeled as a 2D convolution of an original image $f(x, y)$, with a linear time invariant point spread function (PSF) $h(x, y)$, along with some additive noise $n(x, y)$. Typically, research involving the deblurring of an image can be classified as blind or nonblind problems. In the case of nonblind problems, the PSF $h(x, y)$ is assumed to be known. However, in the case of blind deblurring, both the original image and the PSF are unknown. Despite the narrower applicability of the nonblind deblurring approach, it is already a challenging problem, as the convolution operators of interest are typically ill-posed. As a result, this research is ongoing [1–6]. Typical applications of image deblurring lie in various areas of astronomy, optics, and surveillance.

In many scientific applications, the PSF is known. For example in computational photography systems [7], the PSF is known up to a scale. In addition, the PSF due to the camera motion can be effectively estimated from a single image, a sensor image, or through an accelerometer [8,9]. In estimation of the PSF due to one-dimensional motion, affine transformation can be estimated automatically, or through iterations [10–12].

Significant research has been done in the spatial domain. However, in this paper, we propose an alternative approach, which uses geometric moments for nonblind image deblurring. The paper has been organized as follows. An introduction to the blind deconvolution in moment domain is presented with mathematical background in Section 2. Section 3 describes the experimental results, followed by a discussion. The last section concludes this work.

2. Nonblind Deblurring in Moment Domain

In this section, a deblurring algorithm in moment domain and that uses the Euler–Lagrange identity and variational techniques are discussed. A blurred

image possesses higher energy and, therefore, seeks out a lower energy state. Thus, the goal of the variational approach is to construct an energy that describes the quality of the image and then minimize that energy [13]. For this, a well-established theory on partial differential equations (PDE) has been applied. The PDE approach treats an image as a function of space and time, which evolves gradually. Finally, an estimation of the original image can be obtained by iterating the PDE for a fixed number of iterations.

Hence, we begin by using an established relationship between geometric moments for an original and blurred image. Here, the formulation has been discussed for 1D and then extended to 2D. For a 1D N -length signal, $f(x)$, the geometric moment can be computed as

$$m_p^{(f)} = \sum_{x=1}^N x^p f(x). \quad (1)$$

As shown in [14], the relationship between the degraded signal moments with the original signal moments in 1D is given by

$$m_p^{(g)} = \sum_{i=0}^p \binom{p}{i} m_i^{(f)} m_{p-i}^{(h)}, \quad (2)$$

where $m_p^{(g)}$, $m_p^{(f)}$, and $m_p^{(h)}$ are the moments of the degraded signal, original signal, and PSF, respectively, and p is the order of moment. Using Eq. (2), we can now write the energy function, E_p for a specific order, p as

$$E_p = \left(\sum_{i=0}^p \binom{p}{i} m_i^{(\hat{f})} m_{p-i}^{(h)} - m_p^{(g)} \right)^2, \quad (3)$$

where $m_p^{(\hat{f})}$ is the estimated original signal. Taking the derivative of Eq. (3), we obtain

$$\frac{\partial E_p}{\partial m_p^{(\hat{f})}} = 2m_0^{(h)} \left(\sum_{i=0}^p \binom{p}{i} m_i^{(\hat{f})} m_{p-i}^{(h)} - m_p^{(g)} \right). \quad (4)$$

Using the Euler–Lagrange identity, the PDE can be modeled as

$$\frac{\partial m_p^{(\hat{f})}}{\partial t} = - \frac{\partial E_p}{\partial m_p^{(\hat{f})}}. \quad (5)$$

This variational procedure consists of iteratively updating the PDE given in Eq. (5), which is consistent with the gradient descent approach of E_p . Substituting Eq. (4) into Eq. (5) yields:

$$\frac{\partial m_p^{(\hat{f})}}{\partial t} = -2m_0^{(h)} \left(\sum_{i=0}^p \binom{p}{i} m_i^{(\hat{f})} m_{p-i}^{(h)} - m_p^{(g)} \right). \quad (6)$$

Finally, by discretizing Eq. (6), we get

$$m_p^{(\hat{f})}(n+1) = m_p^{(\hat{f})}(n) - 2m_0^{(h)} \Delta t \times \left(\sum_{i=0}^p \binom{p}{i} m_i^{(\hat{f})} m_{p-i}^{(h)} - m_p^{(g)} \right), \quad (7)$$

where n is the number of iterations performed.

Similarly, for the 2D image, Eq. (7) can be generalized as

$$m_{p,q}^{(\hat{f})}(n+1) = m_{p,q}^{(\hat{f})}(n) - 2m_{0,0}^{(h)} \Delta t \times \left(\sum_{k=0}^p \sum_{j=0}^q \binom{p}{k} \binom{q}{j} m_{k,j}^{(\hat{f})} m_{p-k,q-j}^{(h)} - m_{p,q}^{(g)} \right), \quad (8)$$

where p and q are the orders of moments.

Equation (8) is iterated either for a fixed number of iterations or when the error criterion is met. Contrast-to-spatial domain in this equation does not require any regularization term. However, our method needs an additional task of reconstructing the image from $m_{p,q}^{(\hat{f})}$, which can be performed using various techniques available in the literature [15,16].

3. Experimental Results and Discussions

In this section, we first show the validity of the proposed method for 1D signals followed by a comparative analysis with spatial domain. Experiments have been performed on real astronomical images and their perceptual quality has been evaluated through the use of recently introduced quality metrics [17].

A. Deblurring of 1D Signals

To verify our mathematical formulation provided in Eq. (7), we take an example of a 1D signal given as $f(x) = \{2, 1, 4, 3, 5, 1\}$ and the PSF as $h(x) = \{0, 1, 0\}$. The moments of the original image, PSF, and blurred image are obtained using Eq. (1):

$$m_p^{(f)} = \{16, 43, 149, 559, 2213, 9103\}, \quad (9)$$

$$m_p^{(h)} = \{1, 1, 1\}, \quad (10)$$

$$m_p^{(g)} = \{3, 4, 6, 10, 18, 34, 66, 130\}, \quad (11)$$

where p varies from 0 to 5.

By making use of observed blurred image moments, $m_p^{(g)}$ [Eq. (11)] and the moments of the PSF, $m_p^{(h)}$ [Eq. (10)], estimated original image moments, $m_p^{(\hat{f})}$ can be calculated using Eq. (7). From Fig. 1 it can be observed that, after 200 and 30 iterations,

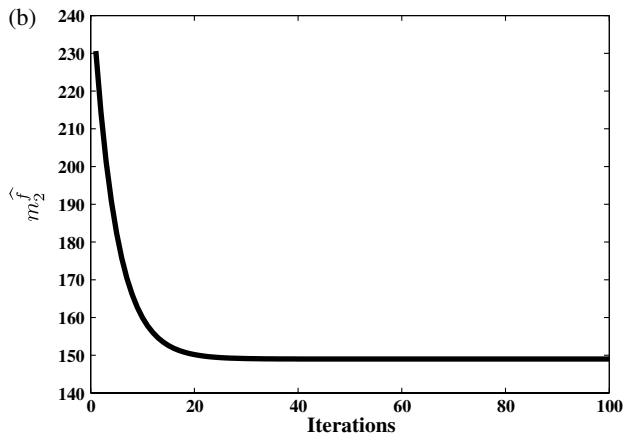
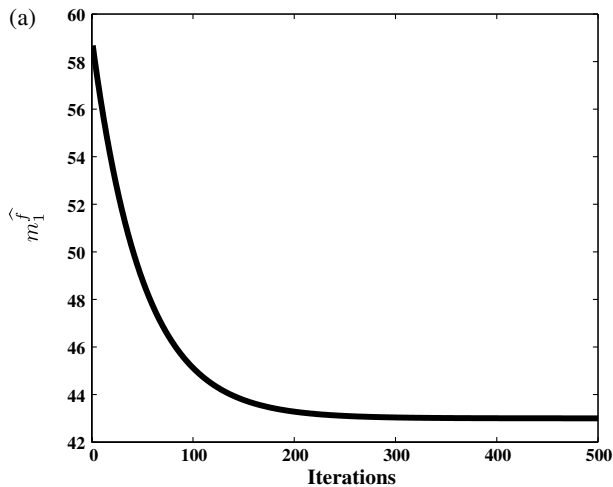


Fig. 1. (a) Estimated $m_1^{\hat{f}}$ and (b) estimated $m_2^{\hat{f}}$.

respectively, the estimated values of $m_1^{\hat{f}}$ and $m_2^{\hat{f}}$ come close to the original image moments of 43 and 149, as calculated in Eq. (9) for $p = 1, 2$.

Hence, the simulation results confirm the validity of the proposed approach in Eq. (7).

B. Deblurring of 2D Images

Further carrying our discussion to 2D image processing, a comparative performance of the proposed work in moment domain with spatial domain is carried out. In this experiment, the original image was blurred using Gaussian PSF. Here, the image size is 32×32 and $p, q = 32$. First, a comparison is performed in terms of how fast the errors in spatial domains $|\hat{f}(x, y) - f(x, y)|$ and $|m_{p,q}^{\hat{f}} - m_{p,q}^{(f)}|$ in moments domain converge. From Fig. 2 it can be observed that the error drops rapidly in the case of moment domain when compared with spatial domain, for a fixed number of iterations. In this paper, the number of iterations performed is 500. If the value of σ used in computation is estimated to be in the range of $\pm 10\%$, then this will affect the aforementioned error. Figure 3 shows the plot of the error with estimated σ . Here, the ideal value of σ is 0.5. Two things can be observed here. First, the variation in the error is greater in the case of spatial domain. Second, with

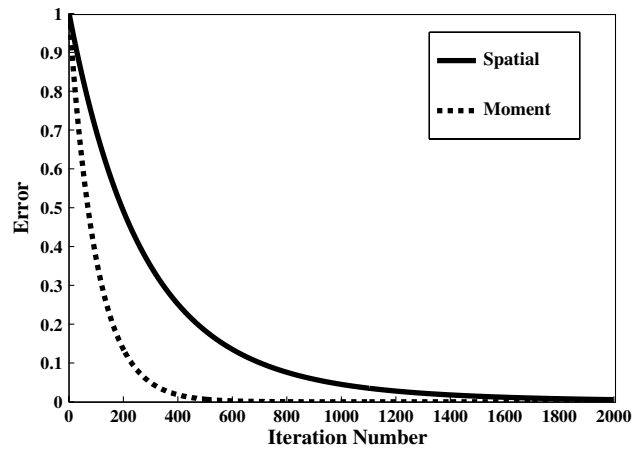


Fig. 2. Error versus iterations.

the regularization parameter, the minimum value of error changes in spatial domain, hence making the quality of an image dependent on the regularization term.

C. Comparative Analysis

A comparative study of the image obtained through both the domains is carried out. In this work, image quality assessment is used to predict perceptual image quality scores without access to reference images. One such technique is known as the Blind/Reference-less Image Spatial Quality Evaluator (BRISQUE) [17], which is used to quantify the quality of an image and gives an objective score. A lower score indicates a higher quality image. Table 1 shows the 32×32 binary image of the letter E and its blurred images. Using this original image, two sets of blurred images were created. In each case the σ and mask size w are $(\sigma = 0.5, w = 5 \times 5)$ and $(\sigma = 1.167, w = 7 \times 7)$, respectively. By applying BRISQUE to each set of blurred images, it can be observed that the objective score obtained using moment domain is less than the spatial domain. Hence, it shows that the perceptual quality of an image is better in the case of moment domain. In the next experiment, we use astronomical images of sizes 64×64 and 128×128 . Two data sets of blurred

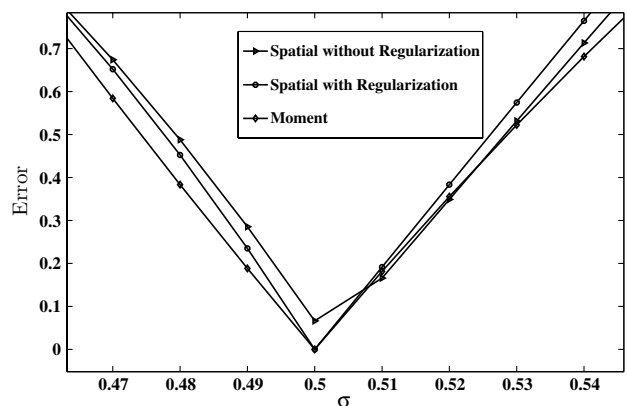


Fig. 3. Error variation with estimated σ .

Table 1. Deblurring Using Spatial and Moment Domain for Binary Images with Different Gaussian Kernel and Mask Size with Corresponding BRISQUE











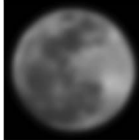

Blurred Images	Deblurred Images		Original Images
	Spatial Domain	Moment Domain	
 $\sigma = 0.5,$ $w = 5 \times 5$ BRISQUE	58.4590	52.4411	
 $\sigma_1 = 1.167,$ $w = 7 \times 7$ BRISQUE	77.2305	71.0035	

Table 2. Deblurring Using Spatial and Moment Domain Approaches for Test Images of Different Size, Gaussian Kernel, Mask Size, with Corresponding BRISQUE

Blurred Images	Deblurred Images		Original Images
	Spatial Domain	Moment Domain	
 $\sigma = 0.833,$ $w = 5$ BRISQUE	31.6582	26.4520	 Size = 64×64
 $\sigma = 2.167,$ $w = 13$ BRISQUE	67.1250	61.6036	 Size = 64×64
 $\sigma = 1.667,$ $w = 7$ BRISQUE	48.2390	42.1376	 Size = 128×128
 $\sigma = 3.167,$ $w = 19$ BRISQUE	75.1275	71.8023	 Size = 128×128

images are created, with ($\sigma = 0.833, w = 5 \times 5$) and ($\sigma = 2.167, w = 13 \times 13$) for 64×64 image, and ($\sigma = 1.667, w = 7 \times 7$) and ($\sigma = 3.167, w = 19 \times 19$) for the 128×128 image. Values of mask size (w) and sigma (σ) are selected on the basis of [18]. Table 2 shows the results of the BRISQUE score for both the spatial and moment domains. It can be seen that the BRISQUE score in the case of the moment domain is less than that for the spatial domain.

4. Conclusion

The main objective of this paper is not to claim that earlier works done in spatial domain are not efficient, but rather explore the moments in the field of deblurring. We presented a novel method of doing nonblind deblurring in moment domain. A mathematical formulation using the Euler-Lagrange identity and variational techniques is proposed to deblur the image in moment domain. An advantage of deblurring the image in moment domain is that it requires less iteration as compared with the spatial domain method and does not need the regularization parameter. A comparative analysis of the results obtained using the spatial and moment domains is conducted using BRISQUE. Experiments demonstrate that better perceptual quality was obtained in moment domain. However, executing PDE in moment domain comes at the cost of large execution time, which can be reduced to some extent using vectorized codes in MATLAB.

We acknowledge the University of Malaya for funding this work. The research has been carried out under HIR grant (UM.C/625/1/HIR/MOHE/ENG/42).

References

1. J. Chen, W. Dong, H. Feng, Z. Xu, and Q. Li, "High quality non-blind image deconvolution using the fields of experts prior," *Optik* **124**, 3601–3606 (2013).
2. M. Almeida and M. Figueiredo, "Parameter estimation for blind and non-blind deblurring using residual whiteness measures," *IEEE Trans. Image Process.* **22**, 2751–2763 (2013).
3. S. Tao, W. Dong, H. Feng, Z. Xu, and Q. Li, "Non-blind image deconvolution using natural image gradient prior," *Optik* **124**, 6599–6605 (2013).
4. S. Tang, W. Gong, W. Li, and W. Wang, "Non-blind image deblurring method by local and nonlocal total variation models," *Signal Process.* **94**, 339–349 (2014).
5. E. Vera, M. Vega, R. Molina, and A. K. Katsaggelos, "Iterative image restoration using nonstationary priors," *Appl. Opt.* **52**, D-102–D-110 (2013).
6. D. S. Stoker, J. Wedd, E. Lavelle, and J. van der Laan, "Restoration and recognition of distant, blurry irises," *Appl. Opt.* **52**, 1864–1875 (2013).
7. R. Fergus, B. Singh, A. Hertzmann, S. T. Roweis, and W. T. Freeman, "Removing camera shake from a single photograph," *ACM Trans. Graph.* **25**, 787–794 (2006).
8. M. Ben-Ezra and S. Nayar, "Motion deblurring using hybrid imaging," in *Computer Vision and Pattern Recognition (IEEE, 2003)*, Vol. **1**, pp. I-657–I-664.
9. L. Yuan, J. Sun, L. Quan, and H.-Y. Shum, "Image deblurring with blurred/noisy image pairs," *ACM Trans. Graph.* **26**, 1–10 (2007).
10. R. Raskar, A. Agrawal, and J. Tumblin, "Coded exposure photography: motion deblurring using fluttered shutter," *ACM Trans. Graph.* **25**, 795–804 (2006).

11. A. Levin, "Blind motion deblurring using image statistics," in *Advances in Neural Information Processing Systems*, B. Schölkopf, J. Platt, and T. Hofmann, eds. (MIT, 2006), pp. 841–848.
12. J. Jia, "Single image motion deblurring using transparency," in *Computer Vision and Pattern Recognition Conference* (IEEE, 2007), pp. 1–8.
13. T. Chan and J. Shen, *Image Processing and Analysis: Variational, PDE, Wavelet, and Stochastic Methods* (Society for Industrial and Applied Mathematics, 2005).
14. J. Flusser, B. Zitova, and T. Suk, *Moments and Moment Invariants in Pattern Recognition* (Wiley, 2009).
15. R. Mukundan, S. Ong, and A. Lee, "Image analysis by Tchebichef moments," *IEEE Trans. Image Process.* **10**, 1357–1364 (2001).
16. P.-T. Yap, R. Paramesran, and S.-H. Ong, "Image analysis by Krawtchouk moments," *IEEE Trans. Image Process.* **12**, 1367–1377 (2003).
17. A. Mittal, A. Moorthy, and A. Bovik, "No-reference image quality assessment in the spatial domain," *IEEE Trans. Image Process.* **21**, 4695–4708 (2012).
18. <http://classes.soe.ucsc.edu/ee264/Fall11/LecturePDF/5-LocalOperations.pdf>.